

PRISM: Probabilistic Runtime Insights and Scalable Performance Modeling for Large-Scale Distributed Training

Alicia Golden^{†‡}, Michael Kuchnik[†], Samuel Hsia[†], Zachary DeVito[†],
Gu-Yeon Wei[‡], David Brooks[‡], Carole-Jean Wu[†]
[†]FAIR at Meta, [‡]Harvard University

Abstract—Large model training beyond tens of thousands of GPUs is an uncharted territory. At such scales, disruptions to the training process are not a matter of *if*, but a matter of *when* – a stochastic process degrading training productivity. Dynamic runtime variation will become increasingly more frequent as training scales up and as GPUs are operated in increasingly power-limited and thermally-stressed environments. At the 64 thousand GPU scale, we already observed 9% GPU time variability for frontier foundation model training. To understand potential causes of variability, we analyze GPU microbenchmarks at scale across a variety of platforms, showing up to a 14% variation in GPU performance on GEMM workloads depending on training hardware and deployed environment.

Motivated by our analysis and the large design space around performance variability, we present PRISM—a performance modeling framework that considers the stochastic nature of the large-scale distributed training. The core of PRISM is the statistical method that provides a quantifiable measure for probabilistic guarantees on training time. Using PRISM, we explore the design and optimization space of distributed training, from parallelization methods to next-generation training systems. PRISM is validated with real-system measurement, showing training time prediction accuracy with 20.8% Kolmogorov-Smirnov distance. Using PRISM, we demonstrate that, depending on computation node placement, up to 1.26× performance improvement potential is available if we factor in sensitivities of parallelization strategies to variation. In addition, we use PRISM to identify kernels to optimize for reducing performance variability and to predict probability of slow-down for large-scale jobs where variation is magnified. We find optimizing communication kernels, such as AllGather and ReduceScatter, contribute most to minimizing variability in training step time.

I. INTRODUCTION

The rapid expansion of large-scale AI – driven by the success of massive Large Language Models (LLMs) – has placed unprecedented demands on distributed training infrastructure. With models like Meta’s LLaMa 4 Behemoth projected to reach two trillion parameters [21], and others such as Google’s Gemini Ultra and OpenAI’s Chat-GPT5 speculated to be upwards of trillions of parameters [25], [33], it is clear the scale of contemporary training jobs is not only computationally intense but also logistically complex. Training these models now requires orchestrating tens of thousands of GPUs across diverse datacenter environments.

While much research has focused on accelerating training through better model architectures [3], [10], [13], [39], [40] or

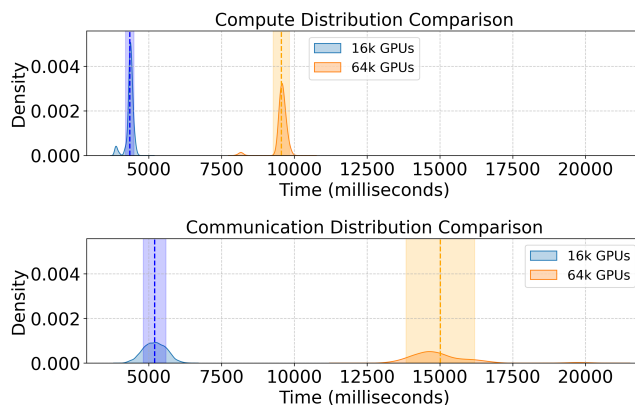


Fig. 1: Distribution of compute and communication time for two LLM training experiments in real-world production training environment – across 16K and 64K+ GPUs respectively. We find the 64K+ job exhibits 2.03× higher standard deviation in compute and 2.91× higher standard deviation in communication operations compared to the 16K job, highlighting increased performance variability at larger scales.

more efficient parallelization strategies [12], [15], [23], [42], comparatively little attention has been paid to a growing factor: system-level variability. In practice, training environments are far from ideal. Even in tightly managed clusters, jobs experience a wide range of performance variation – from hardware faults [17], [20] and thermal throttling [4], [11], [18] to subtle but persistent slowdowns due to clock speed or factors such as garbage collection [20]. This variation is amplified in real-world settings, where jobs are scheduled across thousands of GPUs, and even across heterogeneous nodes.

One under-explored aspect of a dynamic training environment is implicit variability across otherwise homogeneous devices. Even within the same node or DGX system, clock frequency or throttling can lead to consistent disparities across GPUs. While often ignored in small-scale training, these effects can be magnified at-scale, and synchronous operations like AllReduce can be blocked by the slowest device. As we scale to thousands or even millions of GPUs, these small inefficiencies accumulate, contributing to training delays and

resource under-utilization.

Figure 1 characterizes variability in real-world production training environments. We observe in the 64k GPU training experiment $2.03\times$ higher standard deviation in compute and $2.91\times$ higher standard deviation in communication operations per training step compared to that of the 16K job. This highlights the increasing variability seen at larger scales, highlighting the need to optimize in the *presence* of variability.

Existing tools and performance models fall short in addressing this challenge. Most focus on deterministic execution, failing to capture the distributional nature of training behavior under real-world constraints. Moreover, the high cost of large-scale training jobs makes it infeasible to experimentally probe the impact of different sources of variation – training a foundation model such as GPT-4 can cost millions of dollars [7], as well as the opportunity cost of training other models. Yet at the same time, small-scale experiments often fail to capture key components of performance variation. Thus, in this work, we leverage statistical performance modeling to project how workloads perform at-scale.

To bridge this gap, we present **PRISM**: **P**robabilistic **R**untime **I**nsights and **S**calable performance **M**odeling for large-scale distributed training. PRISM combines fine-grained operator-level profiling with statistical modeling techniques to predict not just the mean training time, but the *distribution* of training outcomes under uncertainty. At the core of PRISM is a runtime analysis engine that models each GPU kernel as a probabilistic distribution – measured directly on deployed systems – and propagates these through the training graph using parallelization-aware techniques and Monte Carlo simulation.

We leverage PRISM to explore how variability impacts various aspects of distributed training through a series of four use-cases — analyzing the sensitivity of parallelization strategies to variation for both (i) pipeline parallelism, and (ii) tensor parallelism, as well as (iii) prioritizing which kernels to optimize for reducing performance variability, and (iv) predicting probability of slow-down for large-scale jobs where variation is magnified. Notably, we find optimizing communication kernels such as AllGather and ReduceScatter contribute most to minimizing variability in training step time.

Our work highlights a new design space of variability-aware training systems, as deterministic assumptions about training time may soon no longer hold given the increasing scale and heterogeneous nature of training. Our contributions are as follows:

- We design a series of microbenchmarks to quantify variation across more than twenty thousand GPUs across real-world production datacenter fleet. We find that GEMM kernels can experience as much as 14% variation depending on training hardware and deployed environment.
- We propose PRISM—a variability-aware timing performance modeling framework for large-scale distributed training. PRISM adopts statistical modeling techniques to predict the distribution of model training time.
- We use PRISM to predict how different parallelization strategies respond to variation. We find that the ordering

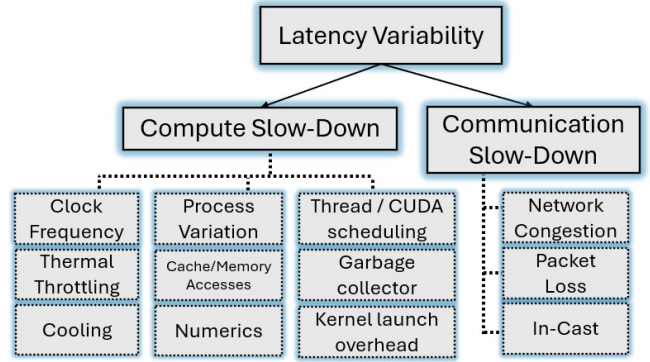


Fig. 2: Taxonomy of Latency Variation. There are a multitude of compute and communication factors that contribute to variability.

of slow GPU ranks in pipeline parallelism can lead to $1.09\times$ difference in training step time.

- We show that increasing scale of training jobs exacerbate the effects of variability, highlighting the importance of variability-aware system design in future datacenter infrastructure.

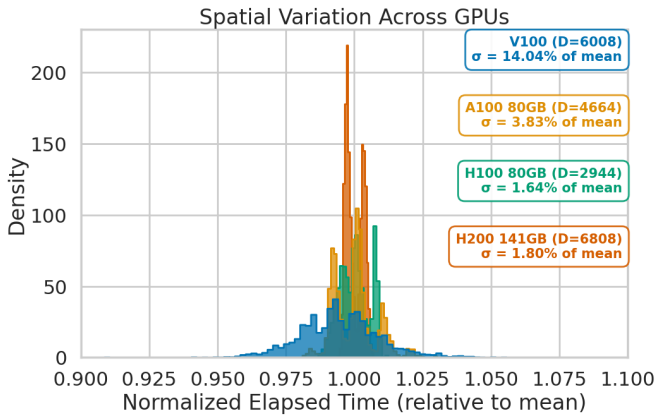
Upon acceptance, we will open-source the PRISM framework to encourage future work in variability-aware optimization for training at-scale.

II. MOTIVATION

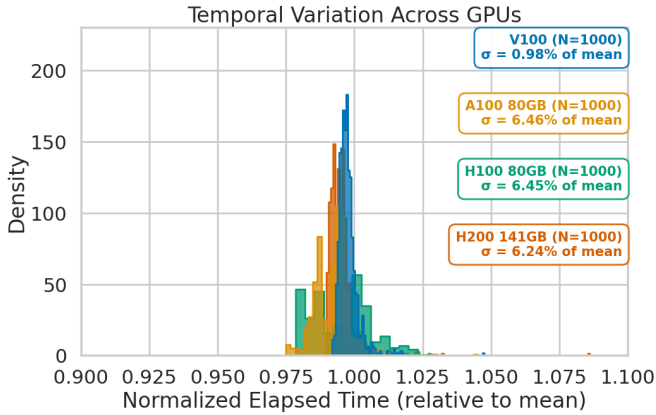
A. Understanding timing variability in real-world training environments

The performance of training at-scale is highly dynamic, subject to variation factors that take many forms. While failures during training can lead to excessive churn at the cluster level that result in lost goodput [17], even failure-free runs are subject to performance variation. For example, when the same neural network computations are executed on the same hardware system repeatedly, the execution time is a stochastic quantity – *temporal timing variability*. In the case of distributed training, where the same neural network computations are run concurrently over a large collection of GPUs or hardware accelerators of other kinds, hardware process variation can lead to further timing performance variability – *spatial timing variability*.

To better understand the sources of variation, we first construct a taxonomy to categorize different forms of performance variation and their potential root causes (see Figure 2). Real-world training jobs experience a wide range of variations of different magnitudes – including variation on seemingly identical GPUs, across different platforms, and failures. Variation on GPUs that are seemingly identical can be caused by a myriad of factors, including varying clock frequency, power throttling, or cooling impacts [24]. Microarchitectural differences can also cause this variation, including cache hits/misses and garbage collection overheads [20]. Numerics is another potential cause



(a) Spatial Timing Variability. Each GEMM kernel is run across $D=2944-6808$ unique GPUs across our clusters. We sample the p50 average value on each GPU and find there exists 1.64-14.04% spatial variation.



(b) Temporal Timing Variability. We profile $N=1000$ iterations of an identical GEMM kernel on the p50 representative GPU across our clusters and find 0.98-6.46% variation.

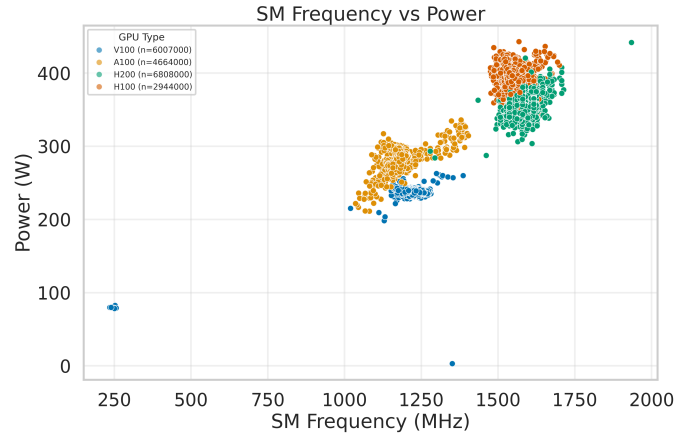
Fig. 3: Significant latency variability is observed for (1) GPUs over the fleet (spatial variability) and (2) execution instances of the same computation kernel on the same GPUs (temporal variability).

of variation, as tensors with many zeros have observed higher speedups due to hardware architectural optimizations [9].

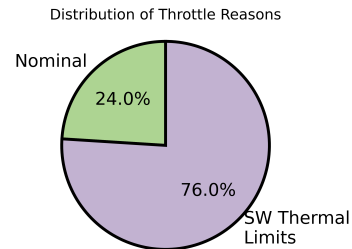
B. Characterizing variability of production clusters.

Taking a step further to quantify the significance of important sources of variation, we characterize three generations of real production training clusters, each equipped with tens of thousands of GPUs. We design microbenchmarks to carefully characterize the *temporal timing variability* and *spatial timing variability* of real production training clusters across GPU generations – including NVIDIA V100, A100, H100, and H200, that were released 7 years apart.

We begin by quantifying spatial timing variability across more than twenty thousand unique GPUs in our production clusters. Figure 3a shows the observed distributions represent-



(a) We observe frequency and power distribution over our GEMM kernels when measuring spatial variation. A100s see a roughly 500 MHz difference in frequency, corresponding to 140W power differential.



(b) Power throttling due to thermal factors is a potential cause of observed variation. Here we show a snapshot of Nvidia’s power throttling codes over the course of measuring $N=1000$ iterations of our GEMM benchmark. We find that 76% of the time, frequency changes due to software thermal limits.

Fig. 4: A significant source of computation latency variability comes from the dynamically varying frequency setting of GPUs.

ing spatial variability across the fleet. We find there exists 1.64-14.04% spatial variation across GPUs for the GEMM kernel.

We then quantify temporal timing variability of the GPUs, using the p50 representative GPU across our clusters. We run each microbenchmark $N=1000$ times on the same GPU and record its variation. As shown in Figure 3b, we observe 0.98-6.46% temporal variation over the microbenchmarks, highlighting the performance variability of individual kernels in a controlled environment.

Delving in more deeply, we observe that a significant source of computation latency variation comes from the dynamically varying frequency setting of GPUs. Figure 4 shows the frequency setting of the GPU streaming multiprocessor (SM) and the corresponding power draw of each GPU while running the microbenchmarks. The majority of runs see a 500 MHz difference in frequency, which corresponds to a 140W power differential. We further observe that power throttling due to thermal factors is a potential cause of observed variation. Figure 3b shows a snapshot of Nvidia’s power throttling

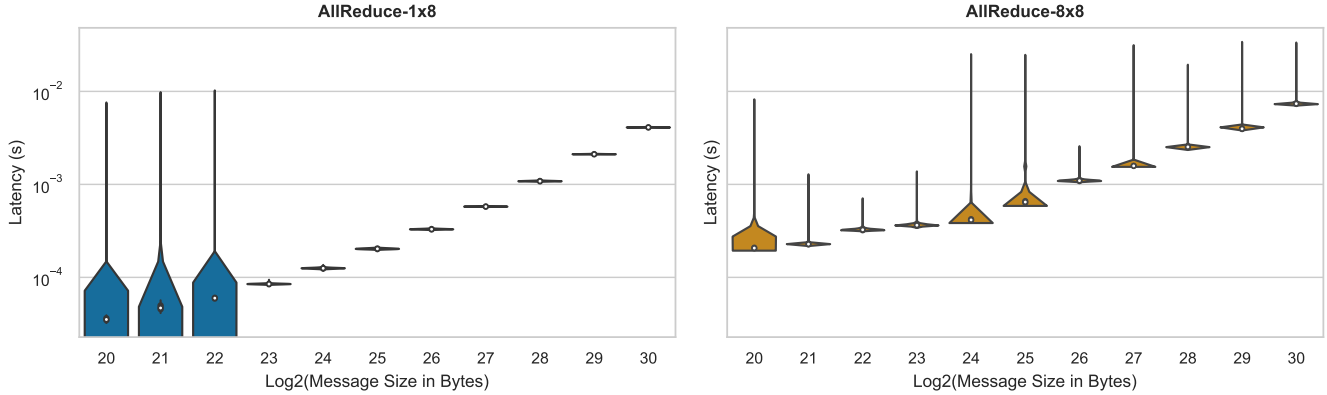


Fig. 5: Communication primitive distributions. Pytorch communication collective AllReduce profiled on 1 and 8 8xH200 GPU nodes across both intra-node NVLink (*left*), and inter-node backend (EFA) network (*right*), respectively. Intra-node communication is nearly deterministic at large message sizes, though we do measure rare stragglers at small message sizes. In contrast, inter-node traffic is more variable—latency fluctuates at a millisecond level and tail latency can span up to an order of magnitude.

codes [24] collected over the course of measuring $N=1000$ iterations of our GEMM benchmark. We find that power is often throttled due to software thermal limits.

Figure 5 characterizes the timing results for communication primitives. We run a series of microbenchmarks to quantify temporal and spatial variability of communication collectives, focusing on AllReduce. We find that inter-node communication collectives exhibit up to an order of magnitude higher tail latency compared to their mean, making communication a significant source of performance variation. While it is difficult to precisely measure the cause of the stragglers, particularly for small message sizes, plausible inter-node causes include network congestion and the measured compounding effects of variability and synchronization at scale. Nevertheless, software communication collectives are heavily utilized during model training, and thus this variability must be accounted for.

C. Optimization in the absence of variability consideration is suboptimal

In order to contextualize this variation, we examine several real-world production model training traces to quantify the level of variation present in the training experiments. Figure 6 shows the distribution of training step time across a 64K+ GPU model training experiment. We find that there exists a significant amount of variation in training step time per GPU, with p5/p50/p95 of 18.6/18.8/19.3 seconds, respectively. We then further examine the variance in communication calls for the same training experiment. We find that AllReduce and ReduceScatter have the highest variance, with p5/p50/p95 of 2.6/3.0/5.7 sec and 1.8/2.4/2.7 seconds, respectively.

Knowing where and why performance variability can come from based on the in-depth real system characterization study on large-scale machine learning training clusters provides us with unique insights for key sources of latency variability to focus mitigation efforts on, in order to provide faster training

time with a tighter bound guarantee. While useful, we still lack the ability to model the impact of performance variations on the overall training performance end-to-end. Our proposed PRISM framework tackles this challenge.

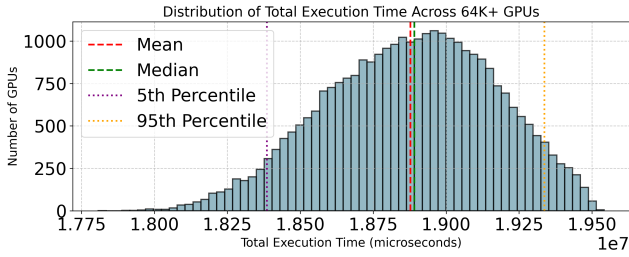
III. PROPOSED DESIGN

We propose PRISM — a performance modeling framework which considers the stochastic nature of the dynamic training environment for large-scale distributed training. Section III-A provides an overview of the framework, Section III-B discusses the framework’s inputs, and Section III-C details our approach to modeling variation at-scale.

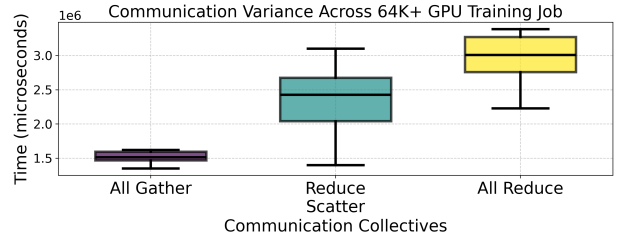
A. Overview of PRISM Framework

PRISM (**P**robabilistic **R**untime **I**nsights and **S**calable **P**erformance **M**odeling for Large-Scale Distributed Training) is a framework for simulating training in the presence of hardware and software variability. Figure 7 depicts the framework. PRISM takes in model architecture, along with a training specification such as the size of the training job, the type of GPUs, parallelism strategy, hardware topology, etc. and predicts training time with a probabilistic guarantee.

To do so, PRISM compiles these inputs into two key structures needed for stochastic modeling: (i) a Directed Acyclic Graph (DAG) capturing workload dependencies, and (ii) operator-level latency distributions profiled on real-hardware. To obtain operator time distributions, we develop a parser that can be used to extract dependencies between operations and isolate individual operators in order to spawn benchmarks that measure variation across various hardware platforms (see Section IV for more details). Once the DAG and operator distributions are collected, we leverage statistical techniques to model the training time, given the presence of variation.



(a) Distribution of training step time across 64K+ GPU LLM trace. We find there exists significant variation in training step time per GPU, with p5/p50/p95 of 18.6/18.8/19.3 seconds.



(b) Variation of communication calls throughout 64K+ GPU training trace. We see that AllReduce and Reduce Scatter have the highest variation, with p5/p50/p95 of 2.6/3.0/5.7 sec and 1.8/2.4/2.7 sec, respectively.

Fig. 6: Observed variation impacts training step time across 64K+ GPU job.

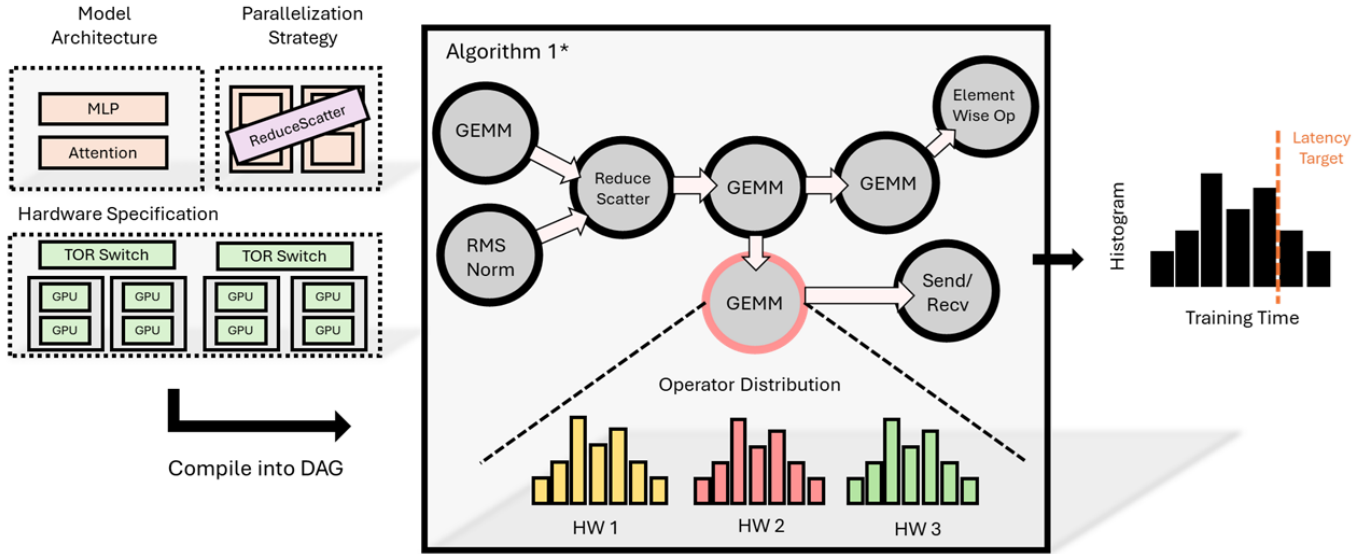


Fig. 7: Overview of PRISM Framework. Given a model architecture, parallelism strategies and training hardware specification, PRISM predicts training time with a probabilistic guarantee.

B. Inputs to PRISM Framework

The PRISM framework takes in several inputs — including model architecture, parallelization strategy, and hardware specifications. We detail each below.

Model Architecture. PRISM requires specification of the model architecture, including the operators and their dependencies. We mainly focus on LLMs following the transformer architecture in this work, although PRISM can be generalized across workloads. Taking an LLM as an example, we input the model definition and dependencies between blocks, as shown.

Parallelization Strategy. PRISM requires knowledge of the parallelization strategy used during training. Parallelization strategy involves how a model is divided over the available compute nodes. Typical model sharding strategies include data parallel (model is replicated, data is sharded) and model parallel (data is replicated, model is sharded). However much work has been done to optimize the partitioning of compute and communication across GPU ranks. Today’s state-of-art

parallelization strategies typically include a hierarchical combination of Data Parallelism (DP), Tensor Parallelism (TP), Pipeline Parallelism (PP), and Context Parallelism (CP) [14], [16], [23], [26], [28], [29], [37], [41], [42].

Tensor Parallelism (TP) is a form of model parallelism that splits a tensor calculation over multiple GPU ranks. TP is often used within a node (i.e., DGX Box) to take advantage of high bandwidth to minimize the costly exposed AllGather and ReduceScatter communication operations.

Pipeline Parallelism (PP) assigns different shards of the model to different GPUs and passes information from one stage to the next. Microbatch scaling is a commonly-used technique to minimize the pipeline bubble, or idle time, spent waiting for data from the previous stage. The effectiveness of pipeline parallelism is often determined by the pipeline schedule used (i.e., 1F1B [16], ZBV [28]), which governs how the forward and backward pass calculations are interleaved across GPUs.

Context Parallelism (CP) is a form of data parallelism designed for long-context LLMs, where each stage operates on a different section of the context [37]. By splitting the model along the sequence length dimensions, CP aims to reduce out-of-memory errors. All pipeline strategies can be specified as a size, indicating how many ranks participate in that group as detailed further in Section IV.

Hardware Specification. Hardware specification and configuration is also necessary as an input to the PRISM framework. The user must specify the hardware platforms they are running on (e.g., V100, A100, H100 GPUs), as well as the topology of the datacenter they are situated in. Datacenter topology is specified by number of compute nodes, networking bandwidth of various links/switches, and relative placement of the compute configuration.

C. Modeling Variability At-Scale with PRISM

In order to accurately model variability at-scale, we must understand the properties of real-world operators and their dependencies. In ML training jobs, operators may either execute (a) sequentially, (b) concurrently, or (c) as part of a pipeline schedule, where compute blocks overlap depending on the schedule design – adding significant complexity to the model.

PRISM captures this variability by characterizing each GPU kernel as a Gaussian distribution, with parameters (mean and sigma) empirically measured from real systems. These individual distributions are then composed to estimate full training time under different execution patterns. We categorize operator interactions into three cases:

- **Serial Execution:** Operators run one after another, with no overlap. Assuming independence, their total time is modeled by summing the means and sum squared of the variance, as shown below:

$$\mu_{\text{total}} = \mu_a + \mu_b + \mu_c \quad (1)$$

$$\sigma_{\text{total}}^2 = \sigma_a^2 + \sigma_b^2 + \sigma_c^2 \quad (2)$$

- **Parallel Execution:** Operators that run concurrently. In this case, we calculate total time through a multiplication of the CDFs F_i of each distribution, equivalent of taking the maximum of values at each point.

$$F_{\text{total}} = F_1 \times F_2 \times \dots \times F_n \quad (3)$$

- **Pipelined Execution:** Operators are scheduled in a pipelined fashion across multiple devices, often overlapping compute and communication. Once the pipeline dependencies and interactions across stages are known, we can leverage Monte Carlo simulation to combine the inherent individual distributions.

We now show how these mathematical formulations can be applied to model uncertainty during LLM training, emphasizing that different parallelization strategies demand distinct modeling approaches. In particular, we utilize a *parallelization-aware approach* to statistical modeling, thus by orchestrating operators where dependencies are known in order to minimize the number of individual elements that the Monte Carlo algorithm has to sample.

Sequential and Parallel Execution Within a GPU. We begin by examining the distribution of operators within a forward and backward pass on a single GPU. Here, we note the interactions between compute and communication primitives, including the fact that there is both exposed and overlapped communication. To analyze this, we recognize the underlying primitives of blocking and non-blocking communication calls. In particular, blocking communication calls can be modeled with serial event execution, whereas non-blocking communication calls are modeled with parallel execution. This is critical to accurately modeling the performance impact of parallelization strategies, such as Tensor Parallelism (TP) and Context Parallelism (CP), where a single GPU’s execution time is impacted by the communication primitives with other GPUs.

PRISM Algorithm 1*

Input: G (Graph)

$$O = \{\mathcal{D}_1, \mathcal{D}_2, \dots, \mathcal{D}_m\}, \mathcal{D}_m \sim \mathcal{N}(\mu_m, \sigma_m^2)$$

Define: $f : (G, O) \mapsto \mathcal{D}_T$

Algorithm:

Initialize $\mathcal{D}_T = \emptyset$

for $r = 1 \dots R$ (num simulations)

 Traverse G . For each node $n \in G$:

 Sample operator $i \sim \mathcal{D}_i \in O$

 If serial dependency:

$$\mu_{\text{total}} = \sum_k \mu_k$$

$$\sigma_{\text{total}}^2 = \sum_k \sigma_k^2$$

 If parallel dependency:

$$F_{\text{total}} = \prod_j F_j$$

 If pipeline dependency:

 continue

 Aggregate sampled times for run r as $t^{(r)}$

$$\mathcal{D}_T \leftarrow \mathcal{D}_T \cup \{t^{(r)}\}$$

 Compute: $\mu_{\mathcal{D}_T} = \mathbb{E}[t], \sigma_{\mathcal{D}_T} = \sqrt{\mathbb{V}[t]}$,

return $\mathcal{D}_T = \{t^{(1)}, t^{(2)}, \dots, t^{(R)}\}, \mu_{\mathcal{D}_T}, \sigma_{\mathcal{D}_T}$.

Output:

$$f(G, O) = \mathcal{D}_T,$$

Parallel Execution Across GPUs. We next look across GPUs, in order to understand how to aggregate timing for various ranks in a distributed training job. At the highest level, multi-GPU execution can be modeled as parallel execution when using Data Parallelism. Typically, each GPU’s execution time, as specified by the compute and communication

dependencies above, can be aggregated together by taking the maximum of the execution times before the synchronization point. However, when modeling distributions, we must multiply the CDFs of each rank’s distribution, in order to quantify the resulting distribution of the DP group.

Pipeline Execution Across GPUs. However, aggregating distributions across GPUs can get significantly more complex when using other parallelization strategies such as Pipeline Parallelism. In this scenario, the pipeline schedule determines which micro batches are operating on a given GPU at any point, and governs the resulting communication dependencies around them. To model this, we codify the dependencies in a DAG, and then run Monte Carlo simulations to sample each individual probability and quantify the resulting distribution.

To model advanced hierarchical parallelization solutions used in state-of-the-art large-scale training, we develop a model for hybrid execution patterns. In particular, we leverage our knowledge of parallelization strategies in order to minimize the sample space of the Monte Carlo simulation. For example, for an LLM training job consisting of tensor parallel, pipeline parallel, and data parallel strategies, we could first aggregate individual operator distributions into a forward and backward pass distribution using parallel and series execution. We then model those distributions with Monte Carlo and our pipeline schedule. And finally, we leverage parallel execution to model the different data parallel ranks.

PRISM therefore captures the intricacies of parallelization strategies when modeling the distribution of training time. Our proposed approach combines real-system latency distributions with profiled dependencies with a framework to aggregate these distributions together in accordance with parallelization strategy to model end-to-end training. Table I summaries common parallelization strategies and their corresponding modeling technique.

TABLE I: Parallelization Strategies and Corresponding Techniques

Parallelization Strategy	Variation Modeling Technique
Data Parallelism	Parallel Execution
Tensor Parallelism	Serial Execution, Parallel Execution
Context Parallelism	Serial Execution, Parallel Execution
Pipeline Parallelism	Monte Carlo Approximation

IV. EXPERIMENTAL METHODOLOGY

In this section, we describe our experimental setup, implementation details, and validation strategy for evaluating the PRISM Framework.

Hardware Setup. We conduct experiments across a diverse set of GPU clusters, including NVIDIA V100, A100, H100, and H200 GPUs. We additionally profile on the latest GB200 systems to evaluate PRISM’s applicability to next-generation hardware. Our experiments focus on large-scale LLM pretraining workloads, such as those based on the LLaMa-4 architecture [21]. Here we introduce the parallelism configurations which is used in the following sections. In particular, we model combinations of Tensor Parallelism (TP),

Pipeline Parallelism (PP), and Data Parallelism (DP) where TP=8, PP=4, and DP=2. We sweep different combinations of these strategies Section V.

Implementation. We implement the PRISM framework in PyTorch, integrating it with custom hooks to profile kernel-level execution times. PRISM models are built using empirical operator-level latency distributions, collected via end-to-end training traces and per-kernel instrumentation.

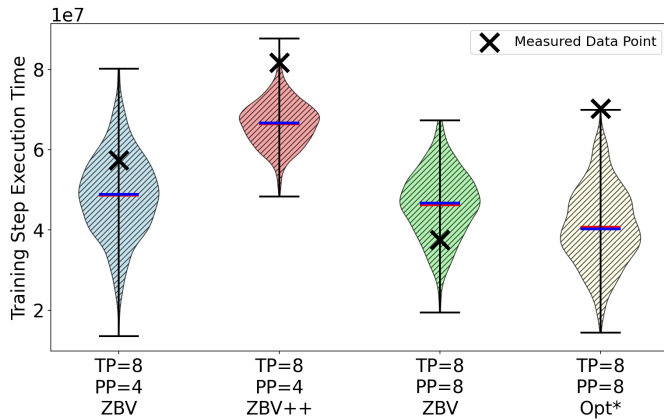
Our profiling framework captures three key components, including (i) module annotations, (ii) input/output shapes of each operator, and (iii) timing information. We then leverage this information to spawn random tensors of the appropriate input shape and benchmarks each operator, gathering additional system data. The input shapes can then be parameterized, and the parser allows the user to subsequently create sweeps for a range of input parameters in order to run unseen benchmarks and construct predictions of new workloads. We additionally extract compute/communication dependencies for given parallelization strategy, which are then represented as a DAG. We implement random sampling and Monte Carlo approximations using packages such as numpy.

Validation. To assess PRISM’s accuracy, we compare its predicted per-step training time against measured time from production training runs. Figure 8 shows results across multiple configurations and scales, comparing actual measurements with PRISM’s Monte Carlo predictions.

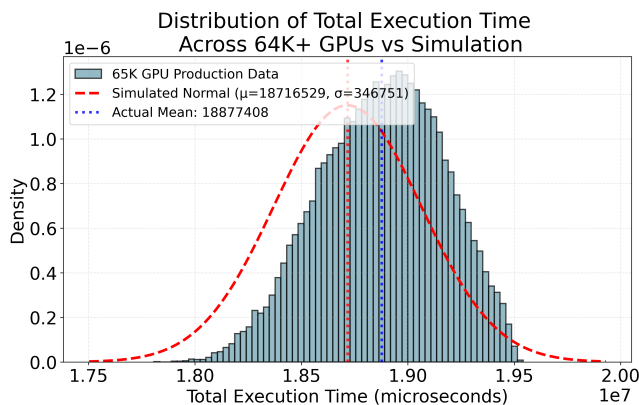
As shown in Figure 8a, we compare PRISM’s predicted distribution with measured datapoints across a sweep of training configurations. These runs are performed with our production workload across 64 H200 GPUs. We vary the tensor parallel (TP) and pipeline parallel (PP) degrees, and also sweep the pipeline parallel schedule across three choices – ZBV, ZBV++, and Opt*. ZBV++ and Opt* represent internal pipeline parallel schedules used in production. For all cases, we find PRISM predicts a representative distribution. It is important to note that running real training jobs at-scale is time-consuming and costly. We are engaged in ongoing efforts to launch more training runs for validation purposes and will update the paper with more datapoints once collected.

Ultimately, we compare the scale-out of our model to the 64K+ GPU production trace, Figure 8b shows the results of this validation. We first randomly sample 20 ranks and use these to quantify the temporal and spatial distribution for individual kernels on a single rank. Then, we plug these distributions into PRISM to predict the training time distribution across 64K+ ranks. We find that PRISM predicts the average execution time within 0.85%. We further compare the distributions and find that PRISM predicts the distribution with 20.8% Kolmogorov-Smirnov distance. Overall, we find that PRISM achieves alignment with observed performance, capturing both mean latency and step-to-step variability.

Modeling overhead. The timing overhead of using PRISM is minimal compared to running full training jobs. Once operator-level traces are collected, PRISM generates step-level predictions on the order of minutes. Monte Carlo simulations are parallelized and scale linearly with the number of samples,



(a) Validation across different parallelization strategy configurations, including different degrees of TP, PP, as well as different pipeline parallel schedules. We find that PRISM captures a realistic distribution for each scenario.



(b) Scale-out validation on 64K+ GPU trace. We sample 20 ranks and quantify spatial and temporal distributions for each kernel, and then use PRISM to project out to 64K+ training job. PRISM predicts the distribution within 20.8% Kolmogorov-Smirnov distance.

Fig. 8: PRISM Validation on real-world training jobs.

making PRISM an efficient way to model large-scale training workloads.

V. EVALUATION RESULTS AND ANALYSIS

We use our proposed performance variability modeling framework to answer a range of key performance tuning and distributed training optimization questions. Section V-A explores use-cases provided for software optimizations, while Section V-B focuses on hardware optimizations, as outlined in Table II.

A. Software Insights from PRISM

1) *Variation Sensitivity of Parallelization Strategy*: We first explore how different sources of variation impact training time under various parallelization strategies. Operator dependencies – such as blocking vs non-blocking communication – mean that variability can propagate through the execution graph

in complex ways. Using PRISM, we model several realistic scenarios encountered during large-scale LLM training.

Research Question I: How does parallelization strategy influence the impact of a random slow node in a distributed training job?

Key Result I: Even one bad node can lead to $1.64\times$ increase in training step time, and depending on computation node placement, up to $1.26\times$ performance improvement potential is available if we factor in sensitivities of parallelization strategies to variation.

Use Case I. Using PRISM, we simulate the impact of random slow nodes in a distributed training job, where all GPUs in that node are affected proportionally. This is representative of scenarios found in production datacenters, such as uneven cooling where certain nodes become excessively hot. We examine the case of our production workload running with a TP=8, PP=4, DP=1 configuration, and leverage PRISM to model slowdown of individual nodes by setting the node of interest at the p95 percentile, while all other nodes run at p50. We note that even one bad node can lead to $1.64\times$ increase in training step time.

Figure 9 showcases that the impact on training iteration time not only depends on the fact that there *is* a slow node, but also *where* it falls in the pipeline. We demonstrate each rank in the training example, highlighting the GPUs set at the p95 distribution in order to observe its placement in terms of parallelization groups. Note with our parallelization configuration mentioned above, 8 ranks constitute one node, which is assigned to a pipeline stage. As shown, we observe that some stage placements of the degraded node lead to significantly worse performance than others, due to compounded pipeline stalls. For example, our results indicate it most advantageous to have the slowest node earliest in the pipeline, as it causes the least amount of stalls. Overall, the ordering of slow ranks can lead to $1.09\times$ difference in training step time.

We subsequently also examine the scenario where we observe slow GPU placement within a TP group, as opposed to across pipeline stages. This is representative of the instance where GPUs in the same node perform unevenly due to chassis layout or localized heat. We highlight this in the right hand side of Figure 9. By keeping the number of p95 ranks constant as compared to the pipeline scenarios, we explore the impact of variation within a TP group. We find that bad node placement within TP groups can see between $1.06\text{--}1.14\times$ more slowdown than variation across pipeline stages. This is due to the fact that TP operations are on the critical path, and thus cannot be easily hidden by other compute/communication events. Overall, across both PP and TP, we find that up to $1.26\times$ performance improvement potential is available if we factor in the sensitivity of these parallelization strategies to variation.

TABLE II: PRISM Modeling Framework and Enabled Research Questions

Research Question
RQ-I: How does parallelization strategy influence the impact of a random slow node?
RQ-II: How does the size of the synchronous group in parallelization strategy influence training time?
RQ-III: Which kernels should be prioritized for optimization to reduce performance variability?
RQ-IV: What is the probability of slow-down, given magnified impact of variation at-scale?

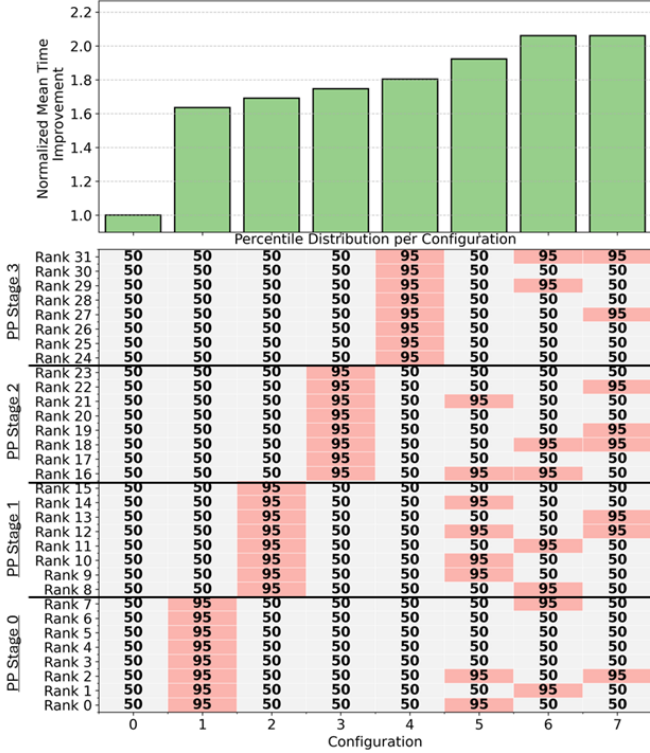


Fig. 9: The ordering of slow nodes can have a significant impact on training time. Here we examine two scenarios: (i) node-level slowdowns, where a slow rank (represented by p95) is found at different stages of the pipeline, and (ii) intra-node imbalance, where those same 8 p95 GPUs are now distributed throughout the TP groups. We find that the ordering of slow ranks can lead to $1.09\times$ difference in training step time.

Research Question II: How does the size of the synchronous group in a parallelization strategy (i.e., TP group) influence the end-to-end training time when variation is taken into account?

Key Result II: Increasing number of ranks in a TP group increases the probability of training slowdown. A 72-rank TP group has an 80% probability of a 4% slowdown, which is $2\times$ more slowdown as compared to a 8-rank group.

Use Case II. Using PRISM, we then explore how changing the size of the synchronous group impacts the execution time’s sensitivity. We start by varying the TP group size while inject random noise into our simulation to model slow ranks. We specifically inject per-GPU variation at a rate of 10%, whereby

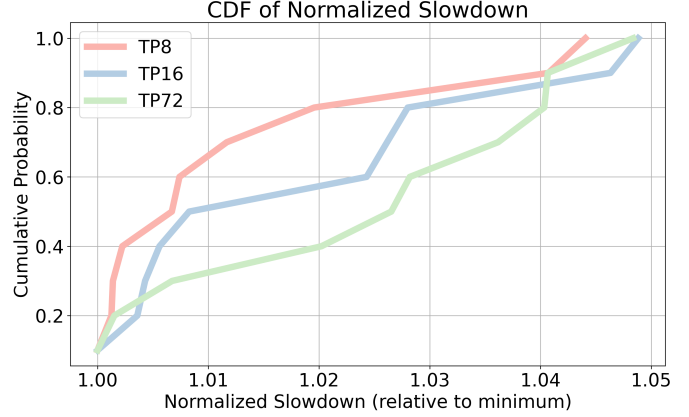


Fig. 10: CDF of normalized slowdown comparing sensitivity to TP group size. We find that the 72-rank TP group has 80% probability of a $1.04\times$ slowdown, whereas the 8- and 16-rank TP groups only experience 80% chance of a $1.02\times$ and $1.028\times$ slowdown, respectively. When magnified across training steps in model execution, this highlights the important role variation can play when scaling to larger TP group sizes.

we set the new mean to be the original p95 distribution value. Figure 10 shows the resulting CDFs of different configurations of TP groups, ranging across 8, 16, and 72 ranks.

PRISM reveals that even modest skew within a TP group can lead to slowdowns, since TP communication during the forward pass is on the critical path. We find that as the number of ranks per TP group are increased, the training run experiences higher probability of slowdown. For example, the 72 rank TP group has a 80% probability of a $1.04\times$ slowdown where as the 8 rank and 16 rank TP groups only experience 80% chance of a $1.02\times$ and $1.028\times$ slowdown, respectively. This impact is then magnified over training steps. This has implications as we consider new infrastructure primitives, like the GB200 72-rank DGX box as compared to the traditional 8-rank DGX box. As more ranks are connected via high-bandwidth fabric, it is natural to re-organize parallelism groups to take advantage of the synchronous operations over fast interconnect. However, we must be mindful of the trade-off of higher variability as we scale to larger synchronous groups.

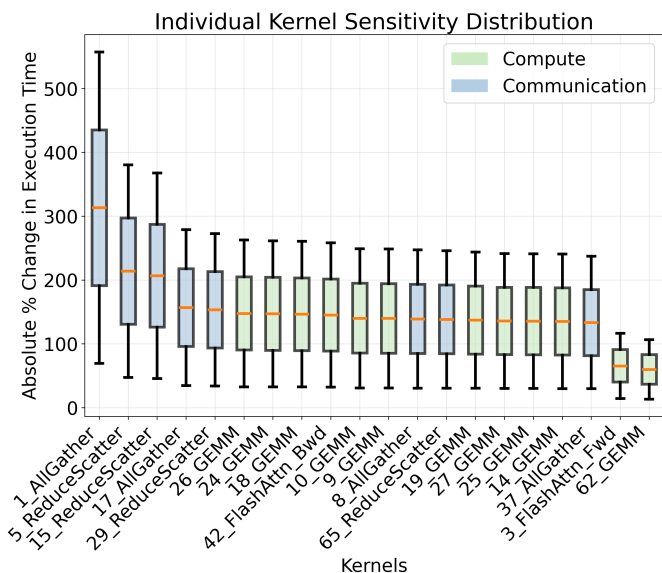


Fig. 11: Impact of individual kernel variation (x-axis) on downstream training iteration time (y-axis). We vary each kernel of interest individually at p95, while holding all others constant at their p50 value. We sweep the amount of variation found in each kernel, and find that training iteration time is most sensitive to communication kernels such as AllGather and ReduceScatter, as well as some GEMM kernels, implying they would be good optimization targets to minimize variation.

2) Kernel Variation Sensitivity Optimization:

Research Question III: Which kernels should be prioritized for optimization to reduce performance variability?

Key Result III: Optimizing communication kernels such as AllGather and ReduceScatter will contribute most to minimizing variability in training step time.

Use Case III. PRISM can model end-to-end sensitivity by injecting additional variance into specific kernels. We observe that even a single unstable kernel can cause significant tail latency, especially if it lies on the critical path of forward or backward computation. Figure 11 shows an example where we select one kernel at a time to perturb, holding all others constant at their p50 value. For the kernel of interest, we hold the mean value of the distribution constant, while sweeping the standard deviation from 5-40%. We then sample the p95 value of the resulting distribution, and calculate the end-to-end training step time with PRISM.

As shown, we find that the sensitivity of training step time varies by kernel. For example, our results indicate that training iteration time is most sensitive to communication kernels, especially AllGather and ReduceScatter, which are often on the critical path of workload execution. We additionally find that a subset of GEMM kernels and the Flash Attention kernel contribute high impact to end-to-end execution time as well. In particular, we note that the Flash Attention backward kernel

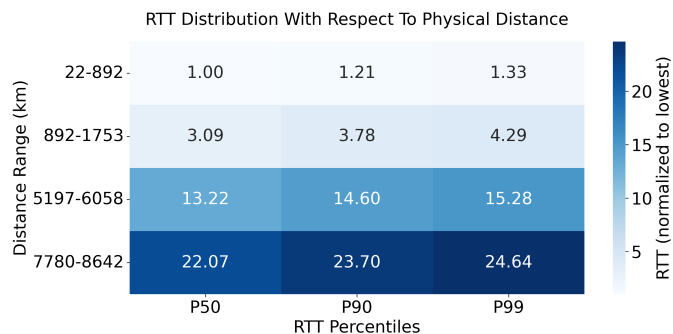


Fig. 12: RTT distribution across datacenters based on their physical distance. Note: we normalize the RTT to p50 to anonymize for proprietary infrastructure measurement results and use the measurement results in the PRISM framework to project the training time performance of distributed training at-scale.

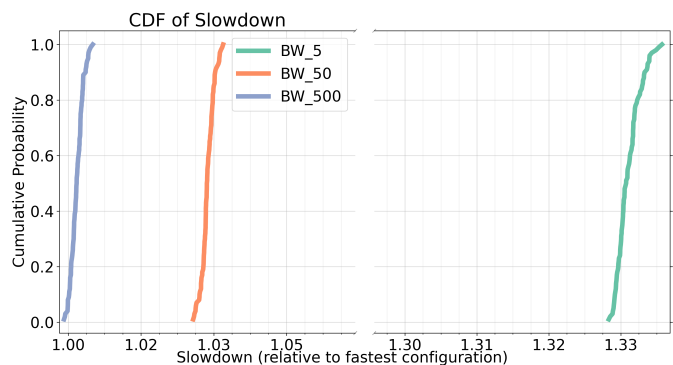


Fig. 13: Sweeping cross-datacenter bandwidth, with distance from pessimistic case in Figure 12. We find that there is a 50% probability that the training job will see a 33% slowdown if using 5 Gbps cross-datacenter link, whereas there is a 80% chance of seeing a 3% slowdown if using 50 Gbps.

results in roughly 100% higher absolute change in execution time than the forward Flash Attention kernel, highlighting the importance of tracing variation through both the forward and backward passes.

Our results indicate that certain kernels are more prone to variation than others, making them natural targets for optimization. For example, optimizing the AllGather and ReduceScatter kernels would contribute most to minimizing variability in training step iteration time.

B. Hardware Insights from PRISM

Research Question IV: What is the probability of slowdown for extremely large-scale GPU training jobs, given the magnified impacts of variation at-scale?

Key Result IV: Increasing variability at-scale impacts performance guarantees for training execution time.

Use Case IV. As training workloads scale to hundreds of thousands of GPUs, small variations compound and can become significant sources of inefficiency. Using PRISM, we extrapolate performance trends under increasing scale. The impact of variation at-scale can be due to two effects: (i) larger number of compute nodes, which increases the possibility that any one node runs at a slower speed than the rest, and (ii) additional hops and varying bandwidths for the network communication, which can introduce additional, significant, variation. We use PRISM to understand the impact of network variability in the cross-datacenter network fabric for large-scale distributed training, for which, pipeline parallelization strategy is used [5].

TABLE III: Scale-Out Parameter Settings

Parameter	Range
Number of Datacenters (N)	2
Distance Between Datacenters (D)	22 - 8642 km
Cross-Datacenter Bandwidth (B_d)	5-400 Gbps [1], [8]
Cross-Cluster Bandwidth (B_c)	400 Gbps [1]
Cross-Rack Bandwidth (B_r)	8×400 Gbps [1]

We model the network effects between real production-scale datacenters by measuring the round trip time (RTT) of the datacenters located in different geographic locations, similar to [2], [6], [22], [27], [30]–[32]. Figure 12 summarizes the measured RTT distribution between the datacenters based on their physical distance. The vertical axis of Figure 12 depicts the physical distance separation between the datacenters for which the measured RTT results are based on while the horizontal axis presents the RTT distribution across p50, p90, and p99. We find that the p50 RTT is more than $22 \times$ longer for the datacenters that are further apart (i.e., between 7780-8642 km) than the datacenters that are physically located closely with each other (i.e., between 22-892km). The network latency’s dependence on the physical distance is expected.

In addition to the RTT, we also have to consider the effect of the network bandwidth capacity between the datacenters for large-scale distributed training. We model the cross-datacenter network using the multi-stage Clos topology common in hyperscalars [1]. We set the bandwidth at the values specified by [1] for cross-rack and cross-cluster links, respectively, amounting to 8×400 Gbps for cross-rack and 400 Gbps cross-cluster. We sweep cross-datacenter bandwidth settings of 5 Gbps (representing a congested scenario), 50 Gbps (representing the capability of existing network technologies), and 400 Gbps (representing the capability of future, more advanced network technologies [8], [36]). Table III summarizes the settings of the network infrastructure.

In order to map the distributed training workload to the cluster topology, we assume Pipeline Parallelism (PP) is the outermost parallelization strategy [5] and thus experiences the burden of cross-building communication. We extract the communication message sizes, and use this in combination with the bandwidth settings to compute transmission delay. We start with our 64k+ GPU trace as input, and extend this to model cross-datacenter communication links.

We plug in the real-system RTT measurement results into PRISM to project the impact of network latency variability on large-scale distributed training. Figure 13 shows the cumulative distribution functions (CDFs) of training time degradation for the different bandwidth settings between the datacenters (Table III) The x-axis represents slowdown as compared to the fastest configuration, whereas the y-axis represents cumulative probability. We find that *there is a 50% probability that the 64k-GPU training job will see a 33% slowdown if using 5 Gbps cross-datacenter link (BW_5), whereas the chance of a 2.9% slowdown is 50% if using 50 Gbps (BW_{50}). The likelihood of training performance degradation is further reduced with a more capable cross-datacenter communication setting (BW_{500}).*

Looking ahead, variability-aware modeling will be critical as large-scale training becomes increasingly distributed. As deployments span multiple datacenters, performance is no longer limited by raw bandwidth alone but is impacted by variability in latency. PRISM’s ability to capture fine-grained variability distributions provides the foundation for more predictable, efficient, and resilient large-scale training systems.

VI. RELATED WORK

A. Large-Scale Training and Performance Modeling

Performance modeling for large-scale training has traditionally relied on analytical abstractions. Systems such as [15], [34] and related works focus on optimizing parallelism strategies under ideal conditions. MADMax [12] introduces a trace-based analytical model to project optimal parallelization strategies while assuming consistent hardware performance regardless of the underlying workload. Although these performance models are effective for making high-level design decisions, they typically assume uniform hardware behavior and thus fail to capture the fine-grained real-world variability that emerges at scale.

Existing non-analytical frameworks, such as Lumos [19] offer detailed statistical profiling capabilities but focus primarily on average case performance. This limits the framework’s ability to model training dynamics in real-world clusters, where mixed GPU generations, thermal variation, and non-uniform interconnects are increasingly common. In contrast, PRISM explicitly models these variations in both space (devices, nodes) and time (runtime), allowing more accurate and realistic predictions for modern and future training workloads.

B. Variability and Failures

A separate body of work has investigated failures in training clusters at-scale, characterizing their frequency of occurrence in production clusters. Papers such as [17] break down the causes of failures and assign probabilities for various root causes. Several recent works have quantified failures and fail-slows at-scale. Most works in this area, such as [20], [35], [38], propose monitoring tools to keep track of slowdowns so that manual intervention can occur. Others also present mitigation strategies. This is orthogonal to our work, which aims to develop a modeling tool for modeling variability at-scale.

Since practitioners often cannot pinpoint where variability originates, it's important to build systems that perform well despite it.

VII. CONCLUSION

Throughout this work, we push the boundaries of traditional datacenter design, challenging traditional assumptions in order to gain insights for next-generation training systems. We present PRISM, a variability-aware framework to explore large-scale heterogeneous training. We then leverage PRISM to explore various scenarios, including the sensitivity of parallelization strategies, kernels, and how variability plays a role in future training scenarios such as cross-datacenter training. Ultimately, variation-aware modeling is essential not just for understanding performance degradation, but for guiding architectural and scheduling decisions that ensure efficient training at-scale.

VIII. ACKNOWLEDGMENTS

The authors would like to thank Bilge Acun, Nellie Wu, and Chien-Yu Lin for their feedback on this work.

REFERENCES

- [1] J. H. Z. Adi Gangidi, "Roce networks for distributed ai training at scale," 2024. [Online]. Available: <https://engineering.fb.com/2024/08/05/data-center-engineering/roce-network-distributed-ai-training-at-scale/>
- [2] M. Adorjan, "Aws region latency matrix," 2025. [Online]. Available: <https://www.cloudping.co/>
- [3] J. Ainslie, J. Lee-Thorp, M. de Jong, Y. Zemlyanskiy, F. Lebron, and S. Sanghai, "GQA: Training generalized multi-query transformer models from multi-head checkpoints," in *Proceedings of the 2023 Conference on Empirical Methods in Natural Language Processing*, H. Bouamor, J. Pino, and K. Bali, Eds. Singapore: Association for Computational Linguistics, Dec. 2023, pp. 4895–4901. [Online]. Available: <https://aclanthology.org/2023.emnlp-main.298/>
- [4] A. Chaudhuri, S. Shukla, S. Bhattacharya, and D. Mukhopadhyay, "'energon': Unveiling transformers from gpu power and thermal side-channels," 2025. [Online]. Available: <https://arxiv.org/abs/2508.01768>
- [5] T. Chen, A. Kubicek, L. Huang, and T. Hoefler, "Crosspipe: Towards optimal pipeline schedules for cross-datacenter training," 2025. [Online]. Available: <https://arxiv.org/abs/2507.00217>
- [6] S. Choi, B. Burkov, A. Eckert, T. Fang, S. Kazemkhani, R. Sherwood, Y. Zhang, and H. Zeng, "Fboss: building switch software at scale," in *Proceedings of the 2018 Conference of the ACM Special Interest Group on Data Communication*, ser. SIGCOMM '18. New York, NY, USA: Association for Computing Machinery, 2018, p. 342–356. [Online]. Available: <https://doi.org/10.1145/3230543.3230546>
- [7] B. Cottier, R. Rahman, L. Fattorini, N. Maslej, and D. Owen, "How much does it cost to train frontier ai models?" 2025. [Online]. Available: <https://epoch.ai/blog/how-much-does-it-cost-to-train-frontier-ai-models>
- [8] Y. Geng, H. Zhang, X. Shi, J. Wang, X. Yin, D. He, and Y. Li, "Delay based congestion control for cross-datacenter networks," in *2023 IEEE/ACM 31st International Symposium on Quality of Service (IWQoS)*, 2023, pp. 1–4.
- [9] A. Golden, S. Hsia, F. Sun, B. Acun, B. Hosmer, Y. Lee, Z. DeVito, J. Johnson, G.-Y. Wei, D. Brooks, and C.-J. Wu, "Is flash attention stable?" 2024. [Online]. Available: <https://arxiv.org/abs/2405.02803>
- [10] A. Gu and T. Dao, "Mamba: Linear-time sequence modeling with selective state spaces," 2024. [Online]. Available: <https://arxiv.org/abs/2312.00752>
- [11] D. Gyawali, "Comparative analysis of cpu and gpu profiling for deep learning models," 2023. [Online]. Available: <https://arxiv.org/abs/2309.02521>
- [12] S. Hsia, A. Golden, B. Acun, N. Ardalani, Z. DeVito, G.-Y. Wei, D. Brooks, and C.-J. Wu, "Mad-max beyond single-node: Enabling large machine learning model acceleration on distributed systems," in *2024 ACM/IEEE 51st Annual International Symposium on Computer Architecture (ISCA)*, 2024, pp. 818–833.
- [13] S. Hsia, U. Gupta, B. Acun, N. Ardalani, P. Zhong, G.-Y. Wei, D. Brooks, and C.-J. Wu, "Mp-rec: Hardware-software co-design to enable multi-path recommendation," in *Proceedings of the 28th ACM International Conference on Architectural Support for Programming Languages and Operating Systems, Volume 3*, ser. ASPLOS 2023. New York, NY, USA: Association for Computing Machinery, 2023, p. 449–465. [Online]. Available: <https://doi.org/10.1145/3582016.3582068>
- [14] Y. Huang, Y. Cheng, A. Bapna, O. Firat, M. X. Chen, D. Chen, H. Lee, J. Ngiam, Q. V. Le, Y. Wu, and Z. Chen, "Gpipe: Efficient training of giant neural networks using pipeline parallelism," 2019. [Online]. Available: <https://arxiv.org/abs/1811.06965>
- [15] Z. Jiang, H. Lin, Y. Zhong, Q. Huang, Y. Chen, Z. Zhang, Y. Peng, X. Li, C. Xie, S. Nong, Y. Jia, S. He, H. Chen, Z. Bai, Q. Hou, S. Yan, D. Zhou, Y. Sheng, Z. Jiang, H. Xu, H. Wei, Z. Zhang, P. Nie, L. Zou, S. Zhao, L. Xiang, Z. Liu, Z. Li, X. Jia, J. Ye, X. Jin, and X. Liu, "Megascala: scaling large language model training to more than 10,000 gpus," in *Proceedings of the 21st USENIX Symposium on Networked Systems Design and Implementation*, ser. NSDI'24. USA: USENIX Association, 2024.
- [16] T. Kim, H. Kim, G.-I. Yu, and B.-G. Chun, "BPipe: Memory-balanced pipeline parallelism for training large language models," in *Proceedings of the 40th International Conference on Machine Learning*, ser. Proceedings of Machine Learning Research, A. Krause, E. Brunskill, K. Cho, B. Engelhardt, S. Sabato, and J. Scarlett, Eds., vol. 202. PMLR, 23–29 Jul 2023, pp. 16639–16653. [Online]. Available: <https://proceedings.mlr.press/v202/kim23l.html>
- [17] A. Kokolis, M. Kuchnik, J. Hoffman, A. Kumar, P. Malani, F. Ma, Z. DeVito, S. Sengupta, K. Saladi, and C.-J. Wu, "Revisiting Reliability in Large-Scale Machine Learning Research Clusters," in *2025 IEEE International Symposium on High Performance Computer Architecture (HPCA)*. Los Alamitos, CA, USA: IEEE Computer Society, Mar. 2025, pp. 1259–1274. [Online]. Available: <https://doi.ieeecomputersociety.org/10.1109/HPCA61900.2025.00096>
- [18] I. Latif, M. A. Shafique, H. Ullah, A. C. Newkirk, X. Yu, and A. Munir, "Cooling matters: Benchmarking large language models and vision-language models on liquid-cooled versus air-cooled h100 gpu systems," 2025. [Online]. Available: <https://arxiv.org/abs/2507.16781>
- [19] M. Liang, H. T. Kassa, W. Fu, B. Coutinho, L. Feng, and C. Delimitrou, "Lumos: Efficient performance modeling and estimation for large-scale LLM training," in *Eighth Conference on Machine Learning and Systems*, 2025. [Online]. Available: <https://openreview.net/forum?id=mwEOLauKI5>
- [20] J. Lin, Z. Jiang, Z. Song, S. Zhao, and M. Yu, "Understanding stragglers in large model training using what-if analysis," in *Proceedings of the 19th USENIX Symposium on Operating Systems Design and Implementation*, 2025.
- [21] Meta, "The llama 4 herd: The beginning of a new era of natively multimodal ai innovation," <https://ai.meta.com/blog/llama-4-multimodal-intelligence/>, 2025.
- [22] R. Mittal, V. T. Lam, N. Dukkkipati, E. Blem, H. Wassel, M. Ghobadi, A. Vahdat, Y. Wang, D. Wetherall, and D. Zats, "Timely: Rtt-based congestion control for the datacenter," *SIGCOMM Comput. Commun. Rev.*, vol. 45, no. 4, p. 537–550, Aug. 2015. [Online]. Available: <https://doi.org/10.1145/2829988.2787510>
- [23] D. Narayanan, M. Shoeybi, J. Casper, P. LeGresley, M. Patwary, V. Korthikanti, D. Vainbrand, P. Kashinkunti, J. Bernauer, B. Catanzaro, A. Phanishayee, and M. Zaharia, "Efficient large-scale language model training on gpu clusters using megatron-lm," in *Proceedings of the International Conference for High Performance Computing, Networking, Storage and Analysis*, ser. SC '21. New York, NY, USA: Association for Computing Machinery, 2021. [Online]. Available: <https://doi.org/10.1145/3458817.3476209>
- [24] NVIDIA, "Nvidia management library (nvml)," in *Nvidia Developer*, 2022. [Online]. Available: <https://developer.nvidia.com/management-library-nvml>
- [25] OpenAI, "Introducing gpt-5," 2025. [Online]. Available: <https://openai.com/index/introducing-gpt-5/>
- [26] S. Pal, E. Ebrahimi, A. Zulfiqar, Y. Fu, V. Zhang, S. Migacz, D. Nellans, and P. Gupta, "Optimizing multi-gpu parallelization strategies for deep learning training," *IEEE Micro*, vol. 39, no. 5, p. 91–101, Sep. 2019. [Online]. Available: <http://dx.doi.org/10.1109/MM.2019.2935967>
- [27] D. Patel, D. Nishball, and J. E. Ontiveros, "Multi-datacenter training: Openai's ambitious plan to beat google's infrastructure,"

2024. [Online]. Available: <https://semianalysis.com/2024/09/04/multi-datacenter-training-openais/>
- [28] P. Qi, X. Wan, G. Huang, and M. Lin, "Zero bubble pipeline parallelism," 2023. [Online]. Available: <https://arxiv.org/abs/2401.10241>
- [29] J. Rasley, S. Rajbhandari, O. Ruwase, and Y. He, "Deepspeed: System optimizations enable training deep learning models with over 100 billion parameters," in *Proceedings of the 26th ACM SIGKDD International Conference on Knowledge Discovery & Data Mining*, ser. KDD '20. New York, NY, USA: Association for Computing Machinery, 2020, p. 3505–3506. [Online]. Available: <https://doi.org/10.1145/3394486.3406703>
- [30] A. Roy, H. Zeng, J. Bagga, G. Porter, and A. C. Snoeren, "Inside the social network's (datacenter) network," *SIGCOMM Comput. Commun. Rev.*, vol. 45, no. 4, p. 123–137, Aug. 2015. [Online]. Available: <https://doi.org/10.1145/2829988.2787472>
- [31] B. Schlinker, I. Cunha, Y.-C. Chiu, S. Sundaresan, and E. Katz-Bassett, "Internet performance from facebook's edge," in *Proceedings of the Internet Measurement Conference*, ser. IMC '19. New York, NY, USA: Association for Computing Machinery, 2019, p. 179–194. [Online]. Available: <https://doi.org/10.1145/3355369.3355567>
- [32] Y.-W. E. Sung, X. Tie, S. H. Wong, and H. Zeng, "Robotron: Top-down network management at facebook scale," in *Proceedings of the 2016 ACM SIGCOMM Conference*, ser. SIGCOMM '16. New York, NY, USA: Association for Computing Machinery, 2016, p. 426–439. [Online]. Available: <https://doi.org/10.1145/2934872.2934874>
- [33] G. Team, "Gemini 2.5: Pushing the frontier with advanced reasoning, multimodality, long context, and next generation agentic capabilities," 2025. [Online]. Available: <https://arxiv.org/abs/2507.06261>
- [34] T. Um, B. Oh, M. Kang, W.-Y. Lee, G. Kim, D. Kim, Y. Kim, M. Muzzammil, and M. Jeon, "Metis: Fast automatic distributed training on heterogeneous GPUs," in *2024 USENIX Annual Technical Conference (USENIX ATC 24)*. Santa Clara, CA: USENIX Association, Jul. 2024, pp. 563–578. [Online]. Available: <https://www.usenix.org/conference/atc24/presentation/um>
- [35] T. Wu, W. Wang, Y. Yu, S. Yang, W. Wu, Q. Duan, G. Yang, J. Wang, L. Qu, and L. Zhang, "Falcon: Pinpointing and mitigating stragglers for large-scale hybrid-parallel training," 2024. [Online]. Available: <https://arxiv.org/abs/2410.12588>
- [36] W. Xia, P. Zhao, Y. Wen, and H. Xie, "A survey on data center networking (dcn): Infrastructure and operations," *IEEE Communications Surveys & Tutorials*, vol. 19, no. 1, pp. 640–656, 2017.
- [37] A. Yang, J. Yang, A. Ibrahim, X. Xie, B. Tang, G. Sizov, J. Reizenstein, J. Park, and J. Huang, "Context parallelism for scalable million-token inference," 2025. [Online]. Available: <https://arxiv.org/abs/2411.01783>
- [38] Z. Yao, P. Hu, C. Miao, X. Jia, Z. Liang, Y. Xu, C. He, H. Lu, M. Chen, X. Li, Z. He, Y. Wang, X. Zou, and J. Jiang, "Holmes: Localizing irregularities in LLM training with mega-scale GPU clusters," in *22nd USENIX Symposium on Networked Systems Design and Implementation (NSDI 25)*. Philadelphia, PA: USENIX Association, Apr. 2025, pp. 523–540. [Online]. Available: <https://www.usenix.org/conference/nsdi25/presentation/yao>
- [39] C. Yin, B. Acun, X. Liu, and C.-J. Wu, "Tt-rec: Tensor train compression for deep learning recommendation models," 2021. [Online]. Available: <https://arxiv.org/abs/2101.11714>
- [40] C. Zhao, C. Deng, C. Ruan, D. Dai, H. Gao, J. Li, L. Zhang, P. Huang, S. Zhou, S. Ma, W. Liang, Y. He, Y. Wang, Y. Liu, and Y. Wei, "Insights into deepseek-v3: Scaling challenges and reflections on hardware for ai architectures," in *Proceedings of the 52nd Annual International Symposium on Computer Architecture*, ser. ISCA '25. New York, NY, USA: Association for Computing Machinery, 2025, p. 1731–1745. [Online]. Available: <https://doi.org/10.1145/3695053.3731412>
- [41] Y. Zhao, A. Gu, R. Varma, L. Luo, C.-C. Huang, M. Xu, L. Wright, H. Shojanazeri, M. Ott, S. Shleifer, A. Desmaison, C. Balioglu, P. Damania, B. Nguyen, G. Chauhan, Y. Hao, A. Mathews, and S. Li, "Pytorch fsdp: Experiences on scaling fully sharded data parallel," 2023. [Online]. Available: <https://arxiv.org/abs/2304.11277>
- [42] L. Zheng, Z. Li, H. Zhang, Y. Zhuang, Z. Chen, Y. Huang, Y. Wang, Y. Xu, D. Zhuo, E. P. Xing, J. E. Gonzalez, and I. Stoica, "Alpa: Automating inter- and Intra-Operator parallelism for distributed deep learning," in *16th USENIX Symposium on Operating Systems Design and Implementation (OSDI 22)*. Carlsbad, CA: USENIX Association, Jul. 2022, pp. 559–578. [Online]. Available: <https://www.usenix.org/conference/osdi22/presentation/zheng-lianmin>